IEEE Access
Multidisciplinary | Rapid Review | Open Access Journal

Received July 17, 2021, accepted August 12, 2021, date of publication August 24, 2021, date of current version September 3, 2021.

Digital Object Identifier 10.1109/ACCESS.2021.3107486

Non-Volatile RF Reconfigurable Antenna on Flexible Substrate for Wireless IoT Applications

TING LENG[1], KEWEN PAN[1,2], XINYAO ZHOU[1], YIZE LI[1], MAHMOUD A. ABDALLA[3], (Senior Member, IEEE), AND ZHIRUN HU[1,4], (Member, IEEE)

[1]Department of Electrical and Electronic Engineering, The University of Manchester, Manchester M13 9PL, U.K.
[2]National Physical Laboratory, Teddington, Middlesex, TW11 0LW, U.K.
[3]Electronic Engineering Department, Military Technical College (MTC) College, Cairo 11787, Egypt
[4]National Graphene Institute, Manchester M13 9PL, U.K.

Corresponding author: Zhirun Hu (z.hu@manchester.ac.uk)

This work was supported by the U.K. Engineering and Physical Sciences Research Council (EPSRC) Engineering Grand Challenge under Grant EP/N010345/1.

ABSTRACT To date semiconductor switches are still the main enablers for electrical circuit and system reconfigurability. They however not only consume dynamic power but also dissipate static power, the former for performing on/off operation and latter for holding on/off state. These semiconductor devices are volatile and not energy efficient due to the need for holding voltage and can significantly increase the system power consumption where hundreds and thousands of switches are needed, such as in large reconfigurable intelligent surfaces and large antenna arrays. In this work, we report a non-volatile reconfigurable antenna that can switch between dual-band at 2.4 GHz and 5 GHz to a single band at 3 GHz. The measured results including reflection, gain and radiation patterns reveal promising performance, experimentally demonstrating a new approach of design and realization of RF switch integrated multi-band reconfigurable antennas. This zero-static power mechanism, along with easy fabrication on the flexible substrates would be very beneficial for Internet of Things (IoT) applications.

INDEX TERMS Switching frequency, telecommunication switching, antennas.

I. INTRODUCTION

In this technology era, the market demands smart wireless connections to support the growing multi-functional and multi-band mobile devices and cloud-based IoT applications [1]–[3]. Reconfigurable antennas have attracted significant attention for their frequency reconfigurability in designing a compact system for IoT applications. These reconfiguration techniques are either based on microelectromechanical systems (MEMS) [4], PIN diodes [5], varactors and photoconductive elements [6] to change the antenna radiating structure, or on the use of materials such as ferrites [7], liquid crystals [8] or tunable resistive materials such as phase transitional material vanadium dioxide (VO_2) [9]. However, apart from MEMS, all these switches have a common limitation: they require DC holding voltage, dissipating static power for their operations [10], [11]. MEMS are however relatively difficult to fabricate and expensive for most RF applications [12]–[15].

On the other hand, the concept of programmable metallization cell (PMC) is introduced as non-volatile switches require no DC hold voltage [16]. This can significantly increase reconfigurable system energy efficiency. Recently, non-volatile RF switches with a parallel plate capacitor structure, referred to as a Metal-Insulator-Metal (MIM) switch have been investigated [17], [18]. Non-volatile chipless RFID tags were made in [19]. In [20], a single frequency band shift antenna on PCB is reported, which uses the MIM switch as reflector/director element for ON/OFF states. Efforts have also been made to fabricate 2D material non-volatile RF switches, but there is no report in integrated antenna applications [15], [10], [21], [22].

This paper reports the design and realization of a non-volatile planar inverted F-shaped monopole antenna fabricated on flexible Kapton substrate with the aim of wearable/flexible IoT applications. The non-volatile RF

The associate editor coordinating the review of this manuscript and approving it for publication was Yuan Yao.

switch is integrated with the antenna structure and the antenna is capable of switching between dual-band at 2.4 GHz and 5 GHz to single band at 3 GHz with no static power supply.

II. ANTENNA DESIGN AND REALIZATION

The antenna uses a planar inverted F-shaped monopole structure, consisting of two resonant line paths responsible for the dual-band behaviour [3]. The lengths of the arms are chosen close to one quarter-wavelength at 2.4 GHz (33 mm) for the Ag layer path and 5 GHz (17 mm) for the Au layer path, respectively. DuPont^{TM} Kapton® HN (125μm) is chosen as the flexible substrate; the film is cleaned firstly in Acetone for 5 mins, then Deionized (DI) water for 2 mins and propan-2-ol (IPA) for 5 mins with ultrasonic bath for better adhesion in later steps. The antenna fabrication started with top part patterning with 200 nm silver using thermal vapor deposition on Kapton film via engraved Nickel shadow mask. Silver is used to act as an active electrode for the non-volatile RF switch. A layer of Nafion is formed uniformly by spin coating the Nafion solution (Sigma Aldrich) at a rate of 5000 RPM for 60 seconds. The sample is then air-dried on a hot plate at 110 °C for 1 min. The Nafion layer is measured to be of 100 nm thickness using stylus profilometer (DektakXT). The lower part of the antenna was patterned with 200 nm Gold as an inert electrode to rule out any switching effect that might arise from interfacial metal oxide formation. An SMA connector is connected to the CPW fed antenna with silver epoxy. The fabrication process is depicted in Fig.1.

Fig. 2 shows the basic structures of the integrated non-volatile reconfigurable antenna. By applying a positive voltage bias, an electric field forms from active to an inert electrode, driving the ions to grow a conductive filament in the ion-conductor layer towards the inert electrode and the switch is in an ON state. On the contrary, a negative bias forms the field of opposite direction; the filament then ruptures, turning the switch to a high resistance state, i.e. the OFF state. Both ON and OFF states do not require any DC power supply to maintain their state.

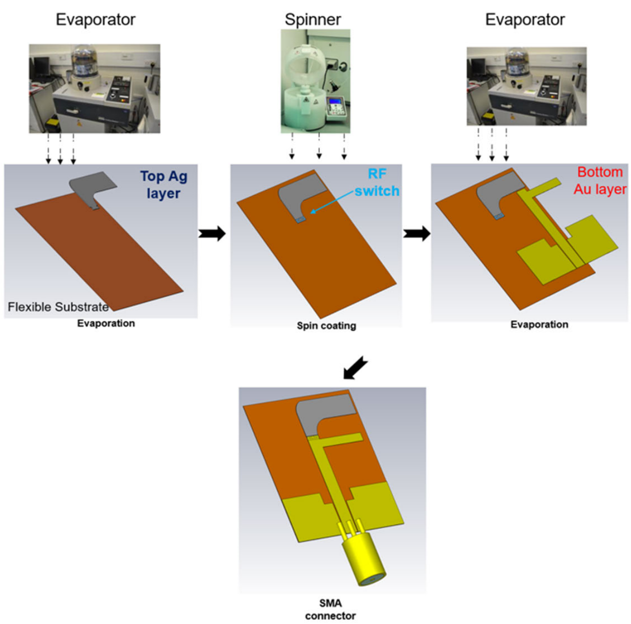

FIGURE 1. The fabrication process of the proposed non-volatile reconfigurable antenna.

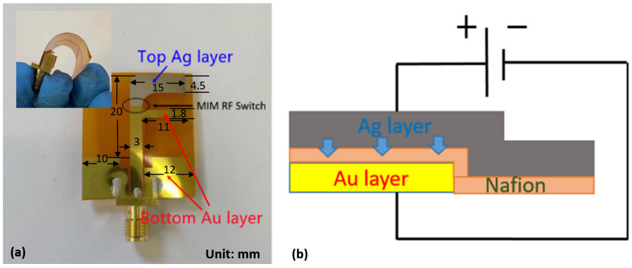

FIGURE 2. Photo and structure of the integrated zero-static power non-volatile reconfigurable antenna. (a) Fabricated reconfigurable antenna with integrated non-volatile RF switch on flexible Kapton substrate; (b) Cross-section of the non-volatile RF switch.

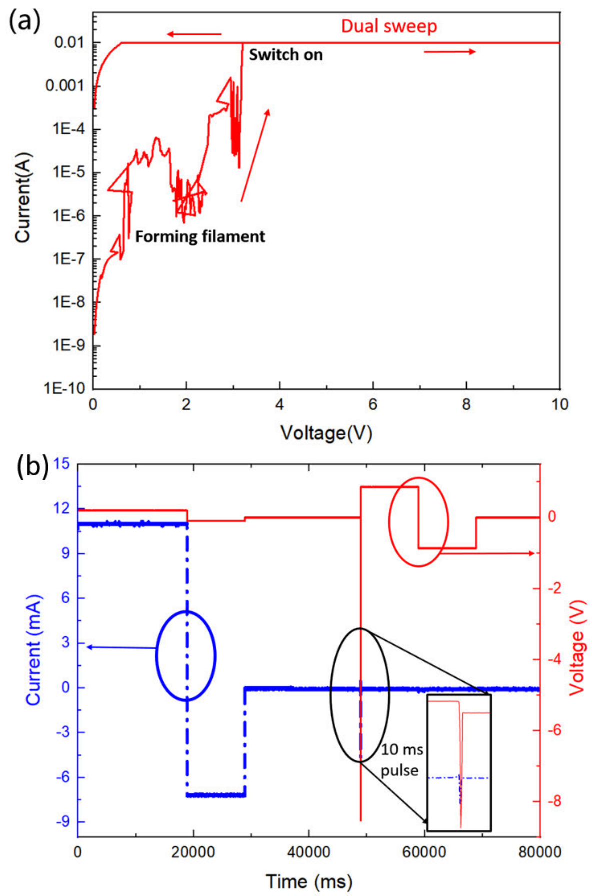

FIGURE 3. DC characteristics of the zero-static power non-volatile RF switch. (a) Applying a positive voltage to switch to ON state; (b) Applying 10 ms voltage pulse (negative) to switch to OFF state.

III. DC MEASUREMENTS

The top and lower part of the antenna is bonded separately with gold wires on a wire bonder (West·Bond 7440E) for DC measurement. The DC performance is measured on a probe

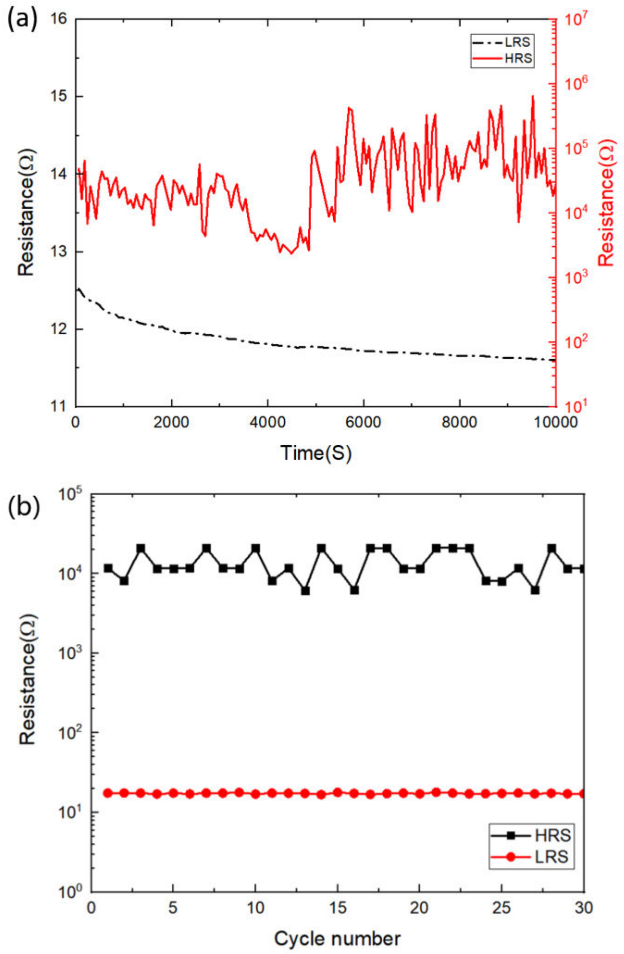

FIGURE 4. Switching performance of the non-volatile RF switch. (a) Time-dependent retention measurements of the switch at room temperature; (b) Resistance distribution of the switch with 30 manual DC switching cycles.

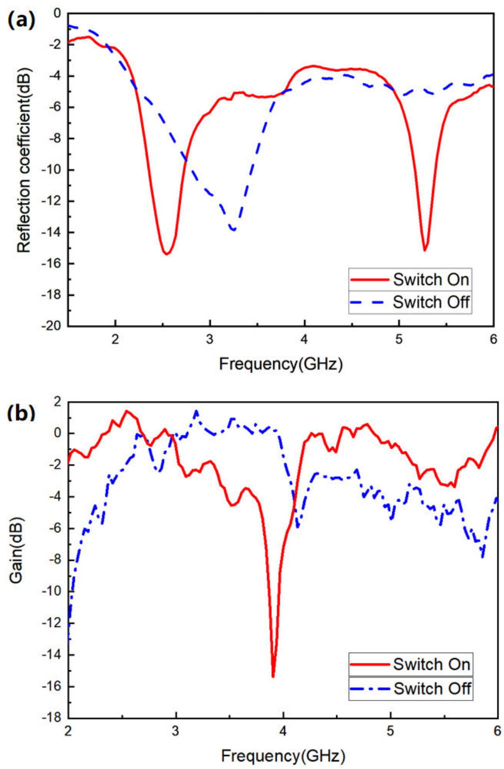

FIGURE 5. Antenna measurement results. (a) Measured reflection coefficient with switch ON/OFF; (b) Measured gain with switch ON/OFF.

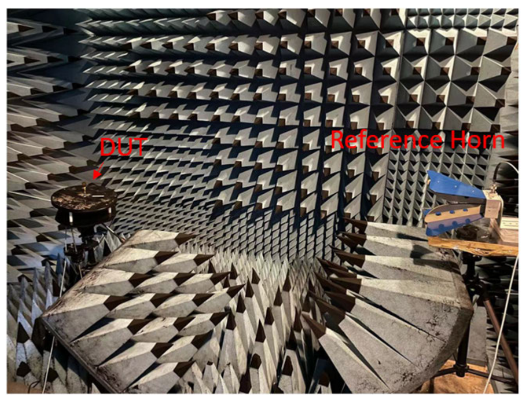

FIGURE 6. Measurement setup in the anechoic chamber.

station (Research Instruments) with Keithley 4200 semiconductor characterization system under ambient conditions as shown in Supplementary Materials Fig. S1.

An 11 mA current compliance was set to minimize the possible damage to the device without affecting the non-volatility (Fig. 3a). By applying a voltage around 3V to the Ag terminal relative to the Au terminal, the current suddenly rises and the RF switch switches on (Fig. 3a). The resistance of the ON state is measured to be less than 15 Ω with a two-probe measurement. The low ON-state resistance value is critical for low-loss non-volatile RF applications. Fig. 3b (before 40,000 ms) shows that how the device behaves during the ON state. The device is firstly applied with a voltage bias of +0.2 V, the current goes to compliance of 11 mA. When a negative voltage bias of −0.1 V is applied, the current becomes −7.1 mA, demonstrating that once the switch is at ON state, it is voltage-dependent like a resistor; positive current when it is positively biased, negative current when negatively biased, and no current when the bias is zero.

When a 10 ms voltage pulse of −8.5 V around 49,000 ms is applied to the switch, it is reset to OFF state. As it can be seen in Fig. 3b, the current then stays still at zero either a positive DC bias or negative one is applied afterward. The enlarged inset shows the voltage pulse. The voltage pulses used to operate the switch are generated from a National Instruments myDAQ and data acquisition with NI USB-6003, the DC bias circuit and schematic is shown in Supplementary Materials Fig. S2. The ON/OFF ratio of the switch is measured to ∼3 orders (Fig. 4b).

Both OFF (high-resistance) and ON (low-resistance) states of the device as a function of time, i.e., the device retention property, have been investigated (Fig. 4a). The device is biased with 0.1 V and the high-resistance state (HRS, R_{OFF}) and low-resistance state (LRS, R_{ON}) resistances are

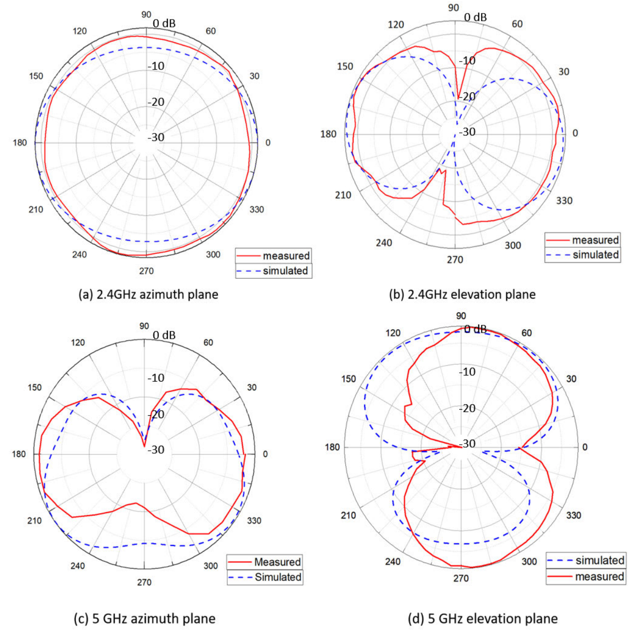

FIGURE 7. Normalized radiation patterns at ON state. (a) 2.4 GHz azimuth plane; (b) 2.4 GHz elevation plane; (c) 5 GHz azimuth plane; (d) 5 GHz elevation plane.

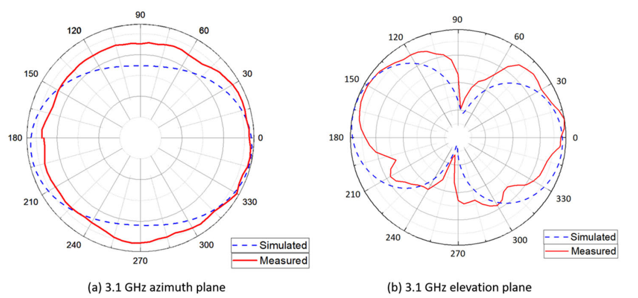

FIGURE 8. Normalized radiation patterns at OFF state and measurement setup. (a) 2.4 GHz azimuth plane; (b) 2.4 GHz elevation plane.

determined by measuring the current with Keithley 4200s semiconductor characterization system.

The measurements are made for every 60 s over 10^5 s time at room temperature. The retention over time reveals the stable operation of the device. A high ON/OFF ratio (∼1000) is also observed. Similar measurements are made after two weeks since the device is fabricated, the results are similar indicating good retention over time.

The endurance of the device was tested by switching between ON/OFF for 30 cycles using the aforementioned DC bias circuit with NI USB-6003 to control and the data were acquired using the LabVIEW program (Fig. 4b).

IV. ANTENNA MEASUREMENTS

The measured reflection coefficient $|S_{11}|$ of the antenna is shown in Fig. 5a using a VNA (Agilent E5071B). It can be seen when the RF non-volatile switch is on, it operates close to the Wi-Fi band (2.4 GHz (2.28–2.53 GHz) and/or 5.0 GHz (4.89–5.05 GHz)). When the switch turns off, it operates

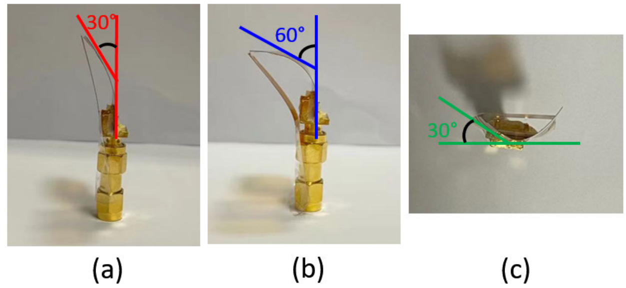

FIGURE 9. Antenna bending illustration (a) Vertical bending 30 degrees (V-30); (b) Vertical bending 60 degrees (V-60); (c) horizontal bending 30 degrees (H).

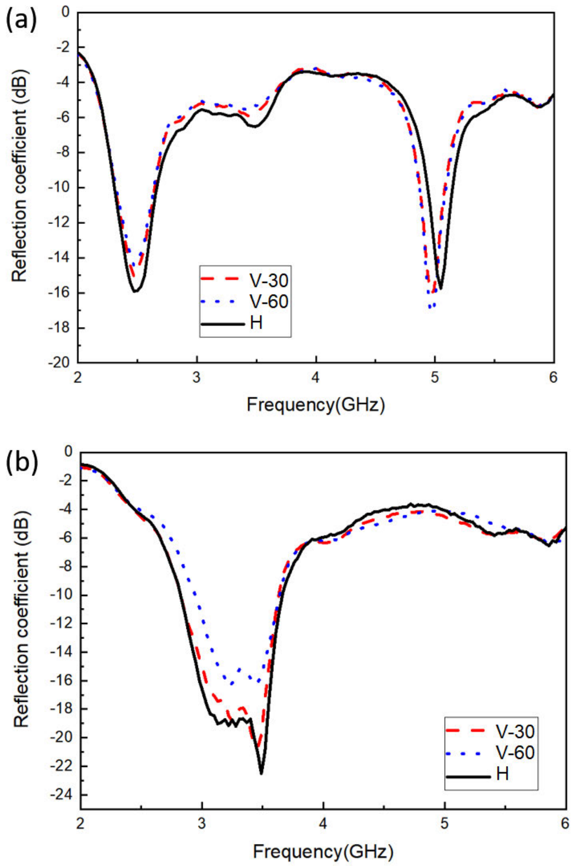

FIGURE 10. Reflection coefficient with vertical bending at 30 degrees (V-30), 60 degrees (V-60), and horizontal bending at 30 degrees (H). (a) ON state; (b) OFF state.

around 5G mid-band 3.5 GHz (2.71–3.59 GHz). The ability to reconfigure around these bands is highly desirable for 5G wireless IoT applications.

Fig. 5b shows the realized gain of the antenna, measured using reference horn antenna Aaronia PowerLOG® 70180. The result coincides with the reflection and the antenna has a positive gain around 2.4 GHz/5 GHz Wi-Fi band when the RF switch is ON. When the switch is OFF, it has a positive gain around 5G mid-band of 3.5 GHz.

To further verify the effective radiation, the radiation patterns of the antenna have been measured in an anechoic

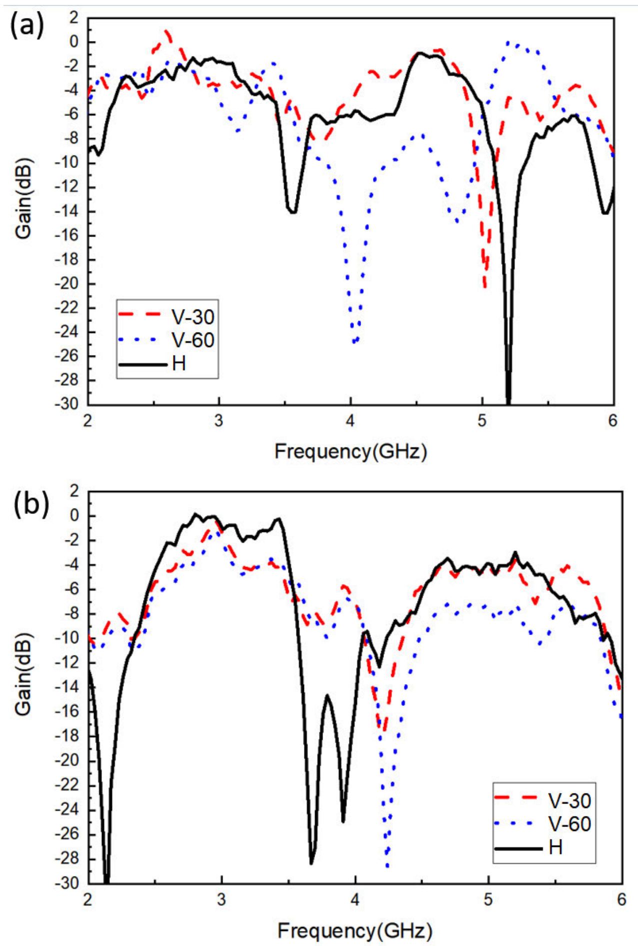

FIGURE 11. Realized Gain with vertical bending at 30 degrees (V-30), 60 degrees (V-60), and horizontal bending (H). (a) ON state; (b) OFF state.

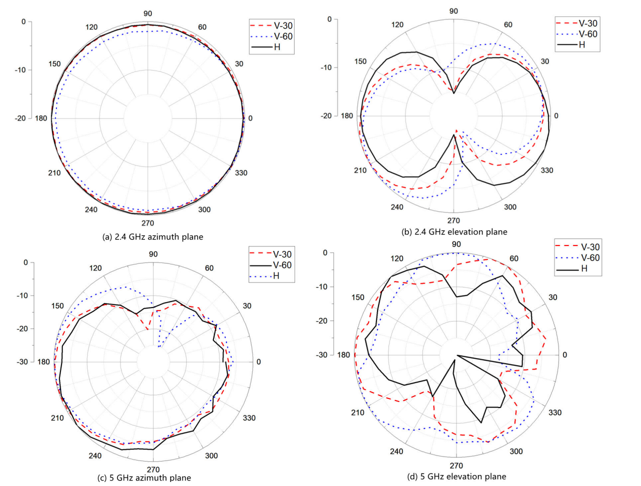

FIGURE 12. Normalized radiation patterns at ON state with vertical bending at 30 degrees (V-30), 60 degrees (V-60), and horizontal bending at 30 degrees (H). (a) 2.4 GHz azimuth plane; (b) 2.4 GHz elevation plane; (c) 5 GHz azimuth plane; (d) 5 GHz elevation plane.

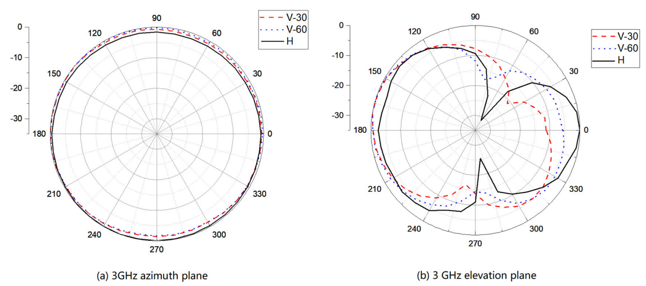

FIGURE 13. Normalized radiation patterns at OFF state with vertical bending at 30 degrees (V-30), 60 degrees (V-30), and horizontal bending at 30 degrees (H). (a) 3 GHz azimuth plane; (b) 3 GHz elevation plane.

chamber (Antenna Measurement Studio 5.5, Diamond Engineering) with a horn antenna (Aaronia PowerLOG® 70180) as a transmitting antenna. The DUT was connected to a rotary table and the data were recorded for every 5°. The antenna gain and radiation pattern measurements of the DUT are measured with a distance of 200 cm apart from the transmitting antenna, shown in Fig. 6, which fulfils the far-field conditions.

From Fig. 7, it can be seen that at 2.4 GHz the antenna has an omnidirectional pattern at the azimuth plane and a dumbbell-like one at the elevation plane, similar to the dipole antenna. At 5 GHz the effective radiation elements of the antenna change, hence the change in the radiation pattern. Fig. 8 shows the radiation patterns when the RF switch is OFF. The azimuth pattern has an oval shape and a bagel-like pattern at the elevation plane. The slight mismatches between the measured and the simulated are possibly due to the SMA connector and the rotary table but the measured results agree with the simulations reasonably well.

V. ANTENNA BENDING PERFORMANCE

The prototype antenna is fabricated on Kapton film, a substrate with great flexibility. Bending tests are made to investigate the antenna radiation performance under different bending positions, vertical bending 30 degrees (V-30), 60 degrees (V-60), and horizontal bending 30 degrees (H) as shown in Fig. 9.

Fig.10 shows the reflection coefficient at ON/OFF state under different bending positions, it is discovered that the bending does not affect antenna matching much, most likely due to the CPW fed monopole antenna structure as reported in [23] and [24]. The measured realized gains of the bent antenna are shown in Fig. 11. The measured gains are inferior to unblended results, which is expected and reasonable due to the bending.

The measured normalized radiation patterns are displayed in Fig. 12 (ON state) and Fig. 13 (OFF state). The shape of the radiation patterns remains consistent with the un-bended scenarios, with a slight change in the vertical bending, where the angle changes as the monopole structure bending to a different angle. Overall, the prototype antenna performs well with a satisfactory result against minor bending; there is no damage or performance degradation when it returned to its normal position. These results show that the RF non-volatile switch integrated reconfigurable antennas on the flexible substrate and the fabrication technique being reported here could have the potential for low-cost and wearable IoT applications.

VI. CONCLUSION

In this paper, we have designed, fabricated, and characterized zero-static power non-volatile RF reconfigurable antenna on a flexible substrate. The measured DC characteristics demonstrate the non-volatility of the switch and the RF experimental data proves the re-configurability. The antenna's operational spectrum can be reconfigured and can radiate effectively. The prototype has also been tested under different bending positions, showing that the reported antenna has a certain level of flexibility. With further development on material selection, device structure, and fabrication process optimization, zero-static power non-volatile RF switches and reconfigurable antennas on the flexible substrate can prove highly desirable for energy-efficient wireless IoT applications.

VII. ACKNOWLEDGMENT

(Ting Leng and Kewen Pan contributed equally to this work.)

REFERENCES

[1] O. Vermesan and P. Friess, Eds., *Internet of Things: Converging Technologies for Smart Environments and Integrated Ecosystems*. Denmark: River Publishers, 2014.
[2] A. I. Al-Alawi, ''WiFi technology: Future market challenges and opportunities,'' *J. Comput. Sci.*, vol. 2, no. 1, pp. 13–18, Jan. 2006.
[3] T. Leng, K. Pan, Y. Jiang, Z. Hu, H. Ouslimani, and M. A. Abdalla, ''Dual band graphene nanoflakes printed compact monopole antenna for low cost WiFi applications,'' in *Proc. IEEE Int. Symp. Antennas Propag. USNC-URSI Radio Sci. Meeting*, Jul. 2019, pp. 1287–1288.
[4] C. D. Patel and G. M. Rebeiz, ''A compact RF MEMS metal-contact switch and switching networks,'' *IEEE Microw. Wireless Compon. Lett.*, vol. 22, no. 12, pp. 642–644, Dec. 2012.
[5] S. Shelley, J. Costantine, C. G. Christodoulou, D. E. Anagnostou, and J. C. Lyke, ''FPGA-controlled switch-reconfigured antenna,'' *IEEE Antennas Wireless Propag. Lett.*, vol. 9, pp. 355–358, 2010.
[6] S. Pendharker, R. K. Shevgaonkar, and A. N. Chandorkar, ''Optically controlled frequency-reconfigurable microstrip antenna with low photoconductivity,'' *IEEE Antennas Wireless Propag. Lett.*, vol. 13, pp. 99–102, Jan. 2014.
[7] Q. Lou, R.-X. Wu, F.-G. Meng, and Y. Poo, ''Realizing frequency reconfigurable antenna by ferrite-loaded half-mode SIW,'' *Microw. Opt. Technol. Lett.*, vol. 59, no. 6, pp. 1365–1371, Jun. 2017.
[8] S. Missaoui, S. Missaoui, and M. Kaddour, ''Tunable microstrip patch antenna based on liquid crystals,'' in *Proc. 21st Int. Seminar/Workshop Direct Inverse Problems Electromagn. Acoustic Wave Theory (DIPED)*, Sep. 2016, pp. 88–91.
[9] D. E. Anagnostou, D. Torres, T. S. Teeslink, and N. Sepulveda, ''Vanadium dioxide for reconfigurable antennas and microwave devices: Enabling RF reconfigurability through smart materials,'' *IEEE Antennas Propag. Mag.*, vol. 62, no. 3, pp. 58–73, Jun. 2020.
[10] R. Ge, X. Wu, M. Kim, J. Shi, S. Sonde, L. Tao, Y. Zhang, J. C. Lee, and D. Akinwande, ''Atomristor: Nonvolatile resistance switching in atomic sheets of transition metal dichalcogenides,'' *Nano Lett.*, vol. 18, pp. 434–441, Jan. 2018.
[11] M. Kim, R. Ge, X. Wu, X. Lan, J. Tice, J. C. Lee, and D. Akinwande, ''Zero-static power radio-frequency switches based on MoS_2 atomristors,'' *Nature Commun.*, vol. 9, no. 1, pp. 1–7, Dec. 2018.
[12] R. Stefanini, M. Chatras, P. Blondy, and G. M. Rebeiz, ''Miniature MEMS switches for RF applications,'' *J. Microelectromech. Syst.*, vol. 20, no. 6, pp. 1324–1335, Dec. 2011.
[13] J. J. Yao, ''RF MEMS from a device perspective,'' *J. Micromech. Microeng.*, vol. 10, no. 4, pp. R9–R38, Dec. 2000.
[14] E. R. Brown, ''RF-MEMS switches for reconfigurable integrated circuits,'' *IEEE Trans. Microw. Theory Techn.*, vol. 46, no. 11, pp. 1868–1880, Nov. 1998.
[15] M. Kim, R. Ge, X. Wu, X. Lan, J. Tice, J. C. Lee, and D. Akinwande, ''Zero-static power radio-frequency switches based on MoS_2 atomristors,'' *Nature Commun.*, vol. 9, no. 1, pp. 1–7, Dec. 2018.
[16] *United States Patent (19) Kozicki (54) PROGRAMMABLE METALLIZATION CELL STRUCTURE AND METHOD OF MAKING SAME Electrochemical Aspects of the Generation of Ramified Metal LIC Electrodeposits Metal Electrocrystallization-an Atomistic View by* in Situ *STM*, Arizona Board Regents Univ. Arizona, Phoenix, AZ, USA, May 1996.
[17] M. P. Jayakrishnan, A. Vena, A. Meghit, B. Sorli, and E. Perret, ''Nafion-based fully passive solid-state conductive bridging RF switch,'' *IEEE Microw. Wireless Compon. Lett.*, vol. 27, no. 12, pp. 1104–1106, Dec. 2017.
[18] J. M. Purushothama, A. Vena, B. Sorli, and E. Perret, ''Electronically re-configurable, non-volatile, nano-ionics-based RF-switch on paper substrate for chipless RFID applications,'' *Technologies*, vol. 6, no. 3, p. 58, Jun. 2018.
[19] M. P. Jayakrishnan, A. Vena, B. Sorli, and E. Perret, ''Solid-state conductive-bridging reconfigurable RF-encoding particle for chipless RFID applications,'' *IEEE Microw. Wireless Compon. Lett.*, vol. 28, no. 6, pp. 506–508, Jun. 2018.
[20] M. P. Jayakrishnan, E. Perret, A. Vena, and B. Sorli, ''Electronically reconfigurable dipole antenna using integrated passive non-volatile solid-state metal-insulator-metal switches,'' in *Proc. IEEE Int. Symp. Antennas Propag. USNC-URSI Radio Sci. Meeting*, Jul. 2019, pp. 303–304.
[21] M. Kim, E. Pallecchi, R. Ge, X. Wu, V. Avramovic, E. Okada, J. C. Lee, H. Happy, and D. Akinwande, ''Non-volatile RF and mm-wave switches based on monolayer hBN,'' in *IEDM Tech. Dig.*, Dec. 2019, pp. 9.5.1–9.5.4.
[22] M. Kim, E. Pallecchi, R. Ge, X. Wu, G. Ducournau, J. C. Lee, H. Happy, and D. Akinwande, ''Analogue switches made from boron nitride monolayers for application in 5G and terahertz communication systems,'' *Nature Electron.*, vol. 3, pp. 479–485, May 2020.
[23] M. E. de Cos and F. Las-Heras, ''Polypropylene-based dual-band CPW-fed monopole antenna,'' *IEEE Antennas Propag. Mag.*, vol. 55, no. 3, pp. 264–273, Jun. 2013.
[24] H. Liu, P. Wen, S. Zhu, B. Ren, X. Guan, and H. Yu, ''Quad-band CPW-fed monopole antenna based on flexible pentangle-loop radiator,'' *IEEE Antennas Wireless Propag. Lett.*, vol. 14, pp. 1373–1377, 2015.

TING LENG received the B.Eng. degree in communication engineering from Coventry University, in 2010, the M.Sc. degree in communication engineering, and the Ph.D. degree in engineering on graphene based electronic and sensing devices from The University of Manchester, in 2012 and 2018, respectively. He learned system-level software and hardware communication theories and analog and digital communications technologies with The University of Manchester. He is currently working as a Research Associate studying sensing properties of graphene and other 2-D materials with the School of Physics and Astronomy, The University of Manchester. He has related publications in major journals and presentations in international conferences. His interests include screen-printed graphene and graphene/2-D materials sensors and electronics.

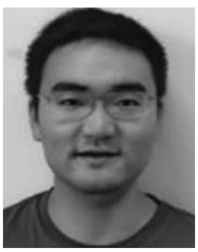

KEWEN PAN was born in Jiangsu, China. He received the B.Eng. degree (Hons.) in electrical and electronic engineering from Nanjing Normal University, Nanjing, China, in 2015, and the Ph.D. degree in electrical and electronic engineering from The University of Manchester, Manchester, U.K., in 2020, focusing on graphene-based microwave device fabrication and characterization.

He has been with the National Physical Laboratory, London, U.K., since December 2020. He has authored/coauthored publications in major journals and international conferences. His research interests include printed graphene antennas and 2-D material-based tunable microwave devices.

XINYAO ZHOU received the B.Eng. degree (Hons.) in electrical and electronic engineering from The University of Manchester, Manchester, U.K., in 2017, where she is currently pursuing the Ph.D. degree.

In 2016, she worked as a Research Assistant with Jilin Electric Power Research Institute. Since 2017, she has been a Teaching Assistant with the Department of Electrical and Electronic Engineering, The University of Manchester. Her research interests include printed graphene antennas, MIMO systems, antenna arrays and beamforming, 2-D conformal microwave devices, and fifth-generation wireless communications. She has related presentations at international conferences.

YIZE LI received the M.Eng. degree (Hons.) from the Department of Electrical and Electronic Engineering, The University of Manchester, Manchester, U.K., in 2020, where he is currently pursuing the Ph.D. degree from the Division of Materials, Devices and Systems, Department of Electrical and Electronic Engineering. His research interests include transparent antenna, graphene/2-D materials RF, and fifth-generation wireless communications.

MAHMOUD A. ABDALLA (Senior Member, IEEE) was born in 1973. He received the B.Sc. and M.Sc. degrees in electrical engineering from the Military Technical College, Cairo, Egypt, in 1995 and 2000, respectively, and the Ph.D. degree from the School of Electrical and Electronic Engineering, The University of Manchester, Manchester, U.K., in 2009. He is currently a Professor and leading the Electromagnetic Waves Group, Electronic Engineering Department, Military Technical College. He has authored more than 200 peer-reviewed journals and conference papers. His research interests include miniaturized, multiband, and wideband microwave/millimeter-wave antennas and components, and also absorbing materials employing metamaterial/EBG structures. He is a Senior Member of URSI and the European Microwave Association (EuMA). He was a recipient of the Egyptian Encouragement State Prize for engineering sciences in 2014 and the Top 1% Publon Worldwide Reviewer Award in 2018 and 2019.

ZHIRUN HU (Member, IEEE) received the B.Eng. degree in telecommunication engineering from Nanjing University of Posts and Telecommunications, Nanjing, China, the master's degree in business administration, and the Ph.D. degree in electrical and electronic engineering from the Queen's University of Belfast, U.K.

He has published more than 250 peer-reviewed journals and conference papers. His current research interests include graphene/2D materials for RF, mmWave and THz communications and sensing applications, wearable electronics, RF, mmWave and THz device, and circuit and antenna design, realization, and characterization.